EVALUATING BOUNDS ON VOLTAGE AND THERMAL SECURITY MARGINS UNDER POWER TRANSFER UNCERTAINTY

Florin Capitanescu
University of Liège
Belgium
capitane@montefiore.ulg.ac.be

Thierry Van Cutsem
FNRS (National Fund for Scientific Research)
University of Liège, Belgium
t.vancutsem@ulg.ac.be

Abstract - This paper deals with the evaluation of bounds on voltage and thermal security margins with respect to contingencies. A margin is the maximal pre-contingency power transfer between either a generation and a load area or two generation areas, such that specified contingencies do not overload lines or make the system voltage unstable. The minimum and maximum margins are computed for given intervals of variations of bus injections. Each bound is the solution of a constrained L_1-norm minimization (or maximization) problem, for which specific algorithms are given. Thermal overloads are handled through linearization, while for voltage stability, fast time simulation and instability mode analysis are used. Nonlinear situations of branch overloads are also considered. The method is illustrated on an 80-bus test system.

Keywords - security assessment, voltage stability, thermal overload, available transfer capability, load power margin

1 INTRODUCTION

INSTABILITY of voltages and thermal overload of transmission equipments (with the associated risk of cascade line tripping) are two significant threats of power systems. While thermal overload has been receiving attention for a long time [1, 2], voltage stability has become in the last two decades a major aspect of power system security [3, 4]. Very often, these two security aspects are analyzed separately, thermal overloads through linear techniques (DC load flow approximation [2, 5]) and voltage instability through nonlinear ones [4]. In some systems, the two aspects can be coupled.

In this paper, we concentrate on security margins defined as the maximum power transfer (between either a load and a generation area or between two generation areas) that can be applied to the system in its current configuration, such that specified contingencies do not cause branch overloads nor voltage instability. There are mature techniques to compute such margins for a given source-sink pattern, defined by the participations of the various bus injections.

In practice, however, the system evolution may be somewhat different from the one assumed in the above calculation. For instance, there is some uncertainty concerning the load increase pattern. Similarly, there is some uncertainty in how generators from external systems will participate to a transaction. This is the case when market rules (still) do not require to disclose such transactions, or with the present-day practice of reserving contractual rather than physical power paths. As security margin computations are reliant on the choice of the source-sink pattern, they are to some extent sensitive to uncertainty on the underlying bus participations.

Therefore, it may be of interest in both operational planning and real time to provide not only the security margin with respect to contingency but also, as a complementary information, the (lower and upper) bounds on this margin for specified ranges of bus injection values. This paper presents methods to compute bounds corresponding to, respectively, the worst and the best source-sink pattern for the contingency(ies) of concern.

Several works have been devoted to determining the minimum distance to the boundary of a feasible space. One of the first method to calculate the closest infeasibility to a given operating point was proposed in the early reference [6]. The feasible region of the injection space was defined as the set of all injections for which the load flow has a solution. A minimum margin was defined and computed using the constrained Fletcher-Powell minimization.

In [7] an iterative and a direct method were proposed to compute the locally closest saddle-node bifurcation to the current operating point in the load power parameter space. The L_2-norm (Euclidian distance) was used to compute the worst-case load increase causing the system to lose equilibrium. More extensive tests with the iterative method were reported in [8], where a Monte-Carlo technique allowed to identify multiple closest bifurcations in some of the test systems. A drawback of the formulation was the independent and unbounded behaviour of the bus active and reactive powers.

The dual problem of maximizing the power transfer between generators and loads was presented in [9], taking into account either voltage stability or voltage quality. Under the assumption that individual loads evolve along a specified direction, the active power generations are varied so as to maximize the power transferred to loads. This L_1-norm maximization problem was solved using a gradient search algorithm.

Insight into the geometry of the bifurcation surface may be found in the above references as well as in [10].

In the meantime, solutions have been proposed to the related problem of optimally changing parameters so as to maximize the distance to saddle-node bifurcation, in the L_2 sense [11, 12]. They are based on the sensitivities of margins to parameters for a given direction of load increase [7, 8, 11].

The case where the feasible region is bounded by inequality constraints (instead of bifurcations as for voltage instability) was considered in [9], for minimum voltage constraints. More recently, [13] proposed a method to find the thermal-constrained interface maximum transfer capability under the worst scenario in generation-load space. The min-max interface transfer is obtained as a bi-level optimization problem whose constrains are derived from the DC load flow equations.

The main contributions of this paper are as follows:
• emphasis is put on contingencies: as indicated above, margins refer to maximum pre-contingency power transfers, such that the system can withstand contingencies;
• minimum and maximum margins are defined with respect to L_1-norm, which (unlike the L_2 one) is directly related to the total power transfer;
• as far as voltage stability is concerned, a fast time-domain method is used to simulate contingencies and obtain the information to adjust the source-sink pattern;
• both thermal overload and voltage instability aspects are considered;
• both generation and load patterns can be varied, though within realistic bounds.

2 STATEMENT OF THE PROBLEM

2.1 System stress

Security margins rely upon the definition of a system *stress*. The latter consists of changes in bus power injections which make the system weaker by increasing power transfer over relatively long distances and/or drawing on reactive power reserves.

Let us denote with P_i the active power injection at the i-th bus ($i = 1, \ldots, n$), which we decompose into:

$$P_i = P_i^o + \Delta P_i^+ - \Delta P_i^- \qquad \Delta P_i^+,\ \Delta P_i^- \geq 0 \qquad (1)$$

where P_i^o is the base case value of the injection, ΔP_i^+ is the additional power *injected into* the network, and ΔP_i^- the one *drawn from* the network, all relative to bus i.

In the sequel, we distinguish between:
(i) a power transfer from a generation to a load area, characterized by:

$$\Delta P_i^+ = \alpha_i\, S \qquad i \in G^+ \qquad (2)$$
$$\Delta P_i^- = \beta_i\, S \qquad i \in L \qquad (3)$$

(ii) a power transfer between two generation areas, characterized by:

$$\Delta P_i^+ = \alpha_i\, S \qquad i \in G^+ \qquad (4)$$
$$\Delta P_i^- = \beta_i\, S \qquad i \in G^- \qquad (5)$$

where S is the total amount of transferred power, (α_i, β_i) are positive real numbers, defining the "direction of stress", G^+ (resp. G^-) is the set of increased (resp. decreased) generators and L the set of increased loads.

With this notation, ΔP_i^+ corresponds to a generation increase only, while ΔP_i^- corresponds to either a load increase (case (i) above) or a generation decrease (case (ii)).

The participation factors are normalized according to:

$$\sum_{i \in L \text{ or } G^-} \beta_i = 1 \quad \text{and} \quad \sum_{i \in G^+} \alpha_i = 1 + \delta \qquad (6)$$

where δ accounts for losses. The latter are thus assumed to vary linearly with S, for simplicity. With this choice, S represented the total power received by the "sinks". In the sequel, it will be referred to as the *system stress*.

Clearly, there are similar expressions for each load reactive power, but we do not make them appear explicitly. In the whole paper, loads are assumed to vary under constant power factor *in the pre-contingency configuration*. If reactive loads would be considered independent, the corresponding equations would be added and straightforwardly handled by the methods described in this paper.

2.2 "Conventional" margins

In usual margin calculations, participation factors (α_i, β_i) are chosen in accordance to (6) and the margin is obtained as the maximum value of the pre-contingency stress S such that the system responds to the contingency in an acceptable way.

Formally, the margin is thus the solution of the optimization problem:

$$\begin{array}{lll} & \max\ S & \\ subject\ to & \mathbf{f}(\mathbf{x}, P_1, \ldots, P_n) = \mathbf{0} & (7) \\ & P_i = P_i^o + \Delta P_i^+ - \Delta P_i^- \quad (i = 1, \ldots, n) & \\ & \Delta P_i^+ = \alpha_i\, S \qquad i \in G^+ & \\ & \Delta P_i^- = \beta_i\, S \qquad i \in L \text{ (or } G^-) & \\ and & \textit{starting from state } \mathbf{x}\textit{, the system has an acceptable response to the contingency.} & \end{array}$$

where (7) stands for the pre-contingency load flow equations, and $\mathbf{x}$ is the pre-contingency operating state.

The above problem can be restated in more mathematical terms, as follows. Consider the space of the ΔP_i^+ and ΔP_i^- variables, as sketched in Fig. 1. At point P, the corresponding values of ΔP_i^+ and ΔP_i^- are used in (1), the load flow equations (7) are solved and the corresponding state $\mathbf{x}$ is used as the initial point of the contingency simulation. According to the system response, P is labelled "secure" or "insecure" for the contingency of concern. Let $\mathcal{S}$ be the sub-space of all points labelled secure.

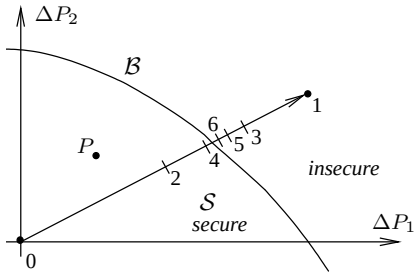

Figure 1: secure region and binary search of margin in a given direction (note: ΔP_i is used indifferently for ΔP_i^+ or ΔP_i^-)

This sub-space is bounded by a surface $\mathcal{B}$, which we assume smooth, and describe - at least formally - by:

$$h(\Delta P_1^+, \ldots, \Delta P_i^+, \Delta P_i^-, \ldots, \Delta P_n^-) = 0 \qquad (8)$$

For a given direction of stress, the margin corresponds to the intersection between $\mathcal{B}$ and the straight line corresponding to (2 - 5), as shown in Fig. 1.

A direct computation of this intersection is possible if (8) can be derived explicitly. This is the case when $\mathcal{B}$ corresponds to branch current constraints under the DC load flow approximation. On the contrary, when a time-domain method is used to simulate the contingency, we can at the most identify on which side of $\mathcal{B}$ a given point is located. In this case, a *binary search* can be used to determine the margin [4, 14]. Figure 1 shows the sequence of points (1,2,...,6) generated by this simple procedure. The latter stops when a secure and an insecure point approach each other by less than some tolerance (points 4 and 6 in the figure). Note that 0 corresponds to the base case (assumed to be secure) and 1 to a maximum stress of interest.

Let $S^\star$ be the maximum stress, corresponding to the margin. We consider now the problem of maximizing (resp. minimizing) $S^\star$ with respect to the α_i's and β_i's.

2.3 Maximum margins

We first eliminate the S and work with the ΔP_i^+ and ΔP_i^- variables only. Summing (3) or (5) over all buses and taking (6) into account yields:

$$\sum_{i \in L \, or \, G^-} \Delta P_i^- = S \tag{9}$$

which shows that it is equivalent to maximize either S or the sum of ΔP_i^-'s. Doing the same with (2, 4, 6) yields:

$$\sum_{i \in G^+} \Delta P_i^+ = (1+\delta)\, S \tag{10}$$

and the last two equations can be combined into:

$$\sum_{i \in G^+} \Delta P_i^+ = (1+\delta) \sum_{i \in L \, or \, G^-} \Delta P_i^- \tag{11}$$

The maximum margin corresponds to the point of surface $\mathcal{B}$ which maximizes the sum of ΔP_i^-'s while satisfying (11). This leads to the optimization problem:

$$\max_{\Delta P_i^+, \Delta P_i^-} \sum_{i \in L \, or \, G^-} \Delta P_i^- \tag{12}$$

$$s.\,t. \quad h(\Delta P_1^+, \ldots, \Delta P_i^+, \Delta P_i^-, \ldots, \Delta P_n^-) = 0 \tag{13}$$

$$\sum_{i \in G^+} \Delta P_i^+ = (1+\delta) \sum_{i \in L \, or \, G^-} \Delta P_i^- \tag{14}$$

$$0 \le \Delta P_i^+ \le B_i^+ \quad i \in G^+ \tag{15}$$

$$0 \le \Delta P_i^- \le B_i^- \quad i \in L \text{ (or } G^-) \tag{16}$$

where the "box" constraints (15,16) have been added to avoid reaching unrealistic load patterns or generation schemes. For loads, the bound B_i^- may be taken as a fraction of the base case power P_i^o. For generators, B_i^- and B_i^+ relate to the generation capacity.

2.4 Minimum margins

Similarly, the minimum margin corresponds to the point of surface $\mathcal{B}$ which minimizes the sum of ΔP_i^-'s while satisfying the same constraints:

$$\min_{\Delta P_i^+, \Delta P_i^-} \sum_{i \in L \, or \, G^-} \Delta P_i^- \tag{17}$$

$$s.\,t. \quad h(\Delta P_1^+, \ldots, \Delta P_i^+, \Delta P_i^-, \ldots, \Delta P_n^-) = 0 \tag{18}$$

$$\sum_{i \in G^+} \Delta P_i^+ = (1+\delta) \sum_{i \in L \, or \, G^-} \Delta P_i^- \tag{19}$$

$$0 \le \Delta P_i^+ \le B_i^+ \quad i \in G^+ \tag{20}$$

$$0 \le \Delta P_i^- \le B_i^- \quad i \in L \text{ (or } G^-) \tag{21}$$

3 BOUNDS ON THERMAL SECURITY MARGINS

3.1 Secure sub-space

When thermal overloads are of concern, the secure sub-space $\mathcal{S}$ is the set of points such that no branch current is above its limit in the post-contingency configuration:

$$I_k^{post} \le I_k^{max} \qquad k = 1, \ldots, b \tag{22}$$

where b is the number of branches, I_k^{post} the post-contingency current in the k-th branch and I_k^{max} the corresponding threshold value.

It is well known that (pre- or post-contingency) branch currents vary almost linearly with bus power injections. The inequality (22) can thus be linearized into:

$$I_{k,\,o}^{post} + \sum_i \frac{\partial I_k^{post}}{\partial P_i} (\Delta P_i^+ - \Delta P_i^-) \le I_k^{max} \qquad k = 1, \ldots, b \tag{23}$$

where $I_{k,\,o}^{post}$ is the post-contingency branch current for the base case value of the injections ($P_i = P_i^o$). The partial derivatives are the sensitivities of the post-contingency branch currents to the pre-contingency injections. They can be determined using the DC load flow approximation [5], or from a well-known sensitivity formula involving the Jacobian of the steady state equations (standard AC load flow or long-term equilibrium equations [4]).

Thus, the boundary $\mathcal{B}$ of the secure region is no longer a smooth function but rather a piece-wise linear one, each linear part of $\mathcal{B}$ corresponding to one of the constraints (23) being active ($\le$ replaced by $=$). Therefore, the formal, smooth equation (8) will have to be replaced by a more appropriate characterization of $\mathcal{B}$.

This is depicted in Figure 2, relative to our previous two-dimensional example. The box constraints (15,16) are shown with thin lines and the boundary $\mathcal{B}$ with heavy lines. The secure area $\mathcal{S}$ is tinted in grey.

With reference to (9), we assume that the objective function is $\Delta P_1 + \Delta P_2$ (shown with dashed lines). Considering that the optimum must lie on $\mathcal{B}$ while obeying the box constraints, one easily verifies that the solution to the $max\ max$ and $min\ max$ problems are the two points shown in the figure.

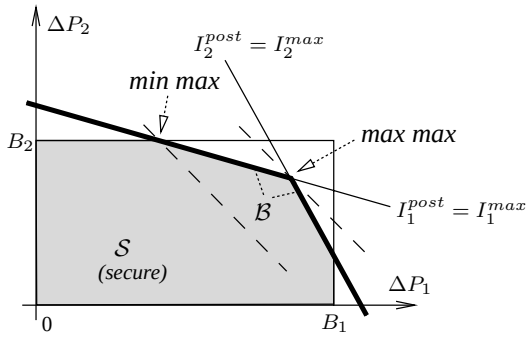

Figure 2: secure sub-space in the linear case

3.2 Maximum margins

As suggested by Fig. 2, the maximum margin is obtained by replacing (8) by the set of inequalities (23) into (12-16), which yields the optimization problem:

$$\max_{\Delta P_i^+, \Delta P_i^-} \sum_{i \in L \, or \, G^-} \Delta P_i^- \tag{24}$$

$$s.\,t. \quad I_{k,\,o}^{post} + \sum_i \frac{\partial I_k^{post}}{\partial P_i}(\Delta P_i^+ - \Delta P_i^-) \leq I_k^{max} \quad k = 1, \ldots, b \tag{25}$$

$$\sum_{i \in G^+} \Delta P_i^+ = (1+\delta) \sum_{i \in L \, or \, G^-} \Delta P_i^- \tag{26}$$

$$0 \leq \Delta P_i^+ \leq B_i^+ \quad i \in G^+ \tag{27}$$

$$0 \leq \Delta P_i^- \leq B_i^- \quad i \in L \text{ (or } G^-) \tag{28}$$

The maximum margin is thus obtained by solving a single Linear Programming (LP) problem. As usual, sparsity programming techniques must be used to preserve computational efficiency. In this respect, small sensitivities may be set to zero.

3.3 Minimum margins

As already mentioned, $\mathcal{B}$ is the union of several linear parts, each relative to a different branch. Denoting one of them by $\mathcal{B}_j$, the minimum of the objective function (9) over the set $\mathcal{B}$ is the smallest among the minima obtained over each subset $\mathcal{B}_j$ separately:

$$\min_{\mathcal{B}} \sum_i \Delta P_i^- = \min_j \left[\min_{\mathcal{B}_j} \sum_i \Delta P_i^- \right]$$

Now, the expression within brackets is the solution of:

$$\min_{\Delta P_i^+, \Delta P_i^-} \sum_{i \in L \, or \, G^-} \Delta P_i^- \tag{29}$$

$$s.\,t. \quad I_{j,\,o}^{post} + \sum_i \frac{\partial I_j^{post}}{\partial P_i}(\Delta P_i^+ - \Delta P_i^-) = I_j^{max} \tag{30}$$

$$\sum_{i \in G^+} \Delta P_i^+ = (1+\delta) \sum_{i \in L \, or \, G^-} \Delta P_i^- \tag{31}$$

$$0 \leq \Delta P_i^+ \leq B_i^+ \quad i \in G^+ \tag{32}$$

$$0 \leq \Delta P_i^- \leq B_i^- \quad i \in L \text{ (or } G^-) \tag{33}$$

(Note that (30) involves a *single equality* while (25) involved b inequalities.)

The procedure is thus the following: for each branch j, solve the above problem to find the minimum margin over the subset $\mathcal{B}_j$, and finally take the smallest among all so found minima.

Note that the above LP problem is very simple (in fact it can be solved without resorting to an LP program, as explained in Section 4.2). For some branches, it may be infeasible. This would correspond, in Fig. 2, to a branch constraint not intersecting the box relative to the B_1 and B_2 bounds. Such a branch can be merely ignored and the enumeration proceeds with the next one. Finally, branches with $I_{k,\,o}^{post} \ll I_k^{max}$ may be also skipped.

3.4 Handling of multiple contingencies

The secure sub-space can be defined with respect to a set of contingencies and minimum (resp. maximum) margins can be computed over this sub-space.

For the maximum margin computation, the set of inequalities (25) is extended to all contingencies, which increases the size of the maximization problem (24-28).

For the minimum margin computation, the size of the minimization problem (29-33) remains unchanged but a different equality (30) has to be considered for all branches and all contingencies, successively.

3.5 Accounting for nonlinear effects

If the $min\ max$ and $max\ max$ points computed from the linear approximations are checked with a more accurate model, it is possible that some branches are overloaded due to the neglected nonlinearities. The latter often result from the voltage drops caused by the increased power transfer.

In such a situation, the sensitivities used in (25) or (30) are corrected. For the k-th branch, the sensitivities are multiplied by $\dfrac{I_k^{real} - I_{k,\,o}^{post}}{I_k^{max} - I_{k,\,o}^{post}}$ where I_k^{real} is the current obtained from the AC load flow calculation. A single new optimization based on the corrected sensitivities is usually enough.

4 BOUNDS ON VOLTAGE SECURITY MARGINS

4.1 Secure sub-space

When voltage instability is of concern, sub-space $\mathcal{S}$ becomes the set of points such that the system responds in a stable way to the contingency. In this case, we build linear approximations of the $\mathcal{B}$ surface, as explained hereafter.

We use Quasi Steady-State (QSS) simulation to determine the system response to contingencies. This well-documented time-domain method [4, 14] is fast and takes into account dynamic effects such as controls acting in the post-contingency configuration.

Moreover, when coupled with small-disturbance analysis, it can extract useful information from unstable cases. Consider, as in Fig. 3, a point U located outside the security region. By definition, when the system initially operates at this point, the post-contingency evolution is voltage

unstable. From the analysis of this evolution one can obtain a reasonably good estimate of the vector $\mathbf{n}$ normal to the $\mathcal{B}$ surface at some point located near U (see Fig. 3). The technique uses sensitivity analysis to detect the critical point, at which the eigenvector relative to the real dominant eigenvalue is computed and therefrom, vector $\mathbf{n}$ [11]. Further details and examples can be found in [15].

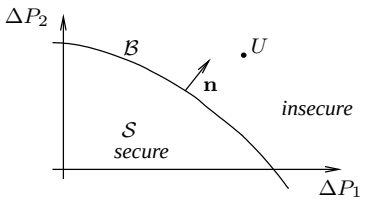

Figure 3: normal vector to boundary surface $\mathcal{B}$

4.2 Minimum margin in the case of a linear $\mathcal{B}$ surface

We show hereafter that in the case of a linear $\mathcal{B}$ surface, the minimum margin can be determined from the components of $\mathbf{n}$ directly.

Consider thus the simple problem, illustrated in Fig. 4, of finding the minimum of $\Delta P_1 + \Delta P_2$ over a single linear boundary $\mathcal{B}$, taking into account the box constraints. Let n_1 and n_2 be the components of the vector normal to $\mathcal{B}$.

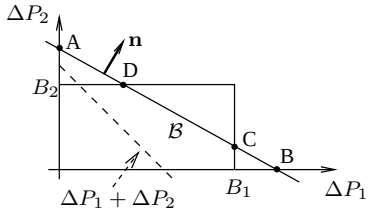

Figure 4: a case of linear $\mathcal{B}$ surface

If the only constraints were $\Delta P_1, \Delta P_2 \geq 0$, the solution would be at point A if $|n_2| > |n_1|$, at point B if $|n_1| > |n_2|$ and at any point of $\mathcal{B}$ is $|n_2| = |n_1|$. In the sequel, we ignore this last case.

If we further impose $\Delta P_1 \leq B_1$ and $\Delta P_2 \leq B_2$, the solution is either C or D, depending again on the relative magnitude of n_1 and n_2.

In the general, n-dimensional case, it can be easily shown that the minimum is such that:
• $\Delta P_i = B_i$ for k variables corresponding to the largest (absolute) components of $\mathbf{n}$
• $\Delta P_i = 0$ for $n - k - 1$ variables corresponding to the smallest components of $\mathbf{n}$. k may vary from 0 to $n - 1$.

4.3 Minimum margins

In Section 2.2 we have described the binary search used to determine the voltage security margin in a given direction (see Fig. 1). We now present a method using the information provided by normal vectors $\mathbf{n}$ to "redirect the stress" in the course of the binary search, with the objective of converging towards the minimum margin. The procedure will be illustrated step-by-step on the simple example of Fig. 5, in which the minimum margin corresponds to point M.

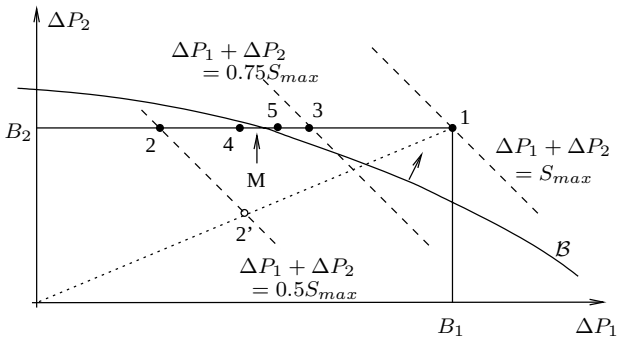

Figure 5: search of the minimum voltage margin

We start by choosing a direction and a maximum stress S_{max}. The corresponding point must fall outside $\mathcal{S}$, in order the system to be unstable and a first normal vector $\mathbf{n}$ to be obtained from the analysis of the unstable evolution. Figure 5 illustrates the case where all ΔP_i's are set to their upper bound B_i.

In a standard binary search the next point to be tested would be 2', corresponding to half stress along the same direction. However, in order to converge to the minimum margin, we change the direction of stress. To this purpose, we approximate $\mathcal{B}$ by a linear surface and apply the result of Section 4.2. Thus, we first sort the various ΔP_i's by decreasing order of their corresponding components of $\mathbf{n}$. Then, following this order, we set the successive ΔP_i's to their bound B_i until their sum exceeds the current level of stress $S_{max}/2$. We adjust the last ΔP_i so that the sum matches $S_{max}/2$ exactly. This leads to point 2 in Fig. 5. At this point we simulate the contingency. The system is stable. No new normal vector is obtained.

We proceed with the $0.75 S_{max}$ stress. In the absence of a new normal vector, we keep the previous ranking of the ΔP_i's. Again, we successively set the ranked ΔP_i's to their bounds B_i and adjust the last one so that the sum equals $0.75 S_{max}$. This leads to point 3. At this point, the system is unstable. A new normal vector is obtained, corresponding to a new linear approximation of $\mathcal{B}$ and providing a new ranking of the ΔP_i's.

The procedure continues in the same way, passing through points 4 and 5 in Fig. 5, until the difference between two successive stresses falls below a tolerance. (Note that the fact that points 2 to 5 all lie on the same line, is a limitation of the two-dimensional example used.)

The following remarks are noteworthy:
• the computational effort is exactly that of a conventional margin computation, for a fixed direction of stress;
• all what matters in this procedure is the *ranking* of the ΔP_i's. In some systems, we have obtained very good results by simply ranking buses according to the values of their voltages. The latter are picked up from one point of the unstable evolution provided by QSS simulation;
• since the method implicitly relies on successive linearizations of the $\mathcal{B}$ surface, the latter should be "smooth enough". On the other hand, changes in $\mathbf{n}$ have no impact as long the ranking of its components is unchanged. This "robustness" is an advantage of the L_1 norm over the L_2 one used in previous works on the subject;
• as already mentioned, loads are changed under constant

power factor. Thus, for each change in active power, there is a change in reactive power. The corresponding components of the $\mathbf{n}$ vectors are combined into a single number, used for ranking. Similarly, we correct the component relative to active power generation to take into account the resulting change in reactive power capability;

• the minimum margin with respect to several contingencies can be obtained by treating each of them separately and taking the lowest among the so found minima.

4.4 Maximum margins

The procedure to obtain maximum margins is similar, except that the ΔP_i's corresponding to the smallest components of $\mathbf{n}$ are the first to be changed. The handling of several contingencies is not detailed here due to space limitations.

5 ILLUSTRATIVE EXAMPLES

5.1 System and power transfers

We consider the 80-bus system shown in Fig. 6, a variant of the "Nordic 32" system used e.g. by CIGRE Task Force 32.02.08 on Long-Term Dynamics (1995). A rather heavy power transfer takes place from the "North" to the "South" areas (see figure).

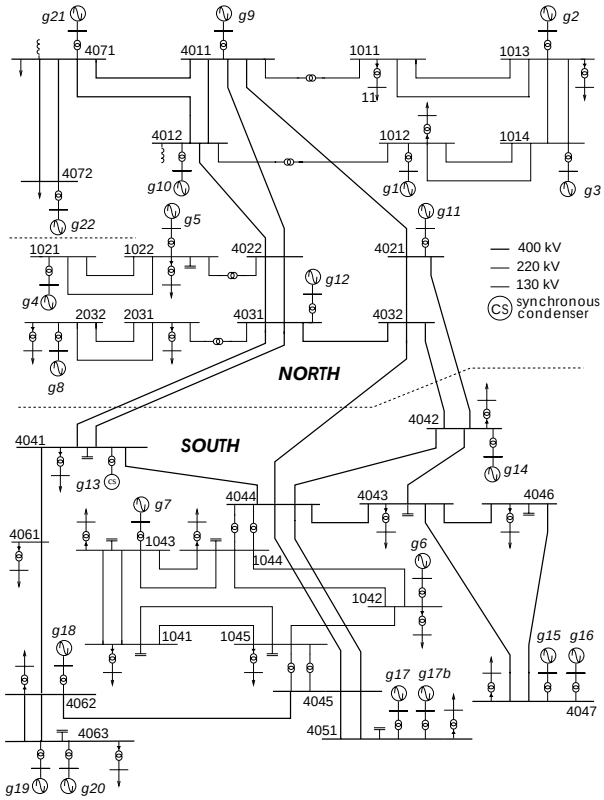

Figure 6: the (slightly modified) "Nordic 32" system

The QSS long-term simulation reproduces the dynamics of load tap changers and overexcitation limiters[4]. Generators respond to a disturbance according to governor control. The Southern generators having infinite speed droops, any power imbalance is covered by Northern generators, which adds to the North-South power flow.

We consider two power transfers:

I. *Generation to Load* (denoted GL in the sequel): a load increased in the South area ($S_{max} = 600$ MW/ 180 MVAr) is covered by a generation increase in the North one ($S_{max} = 630$ MW, accounting for losses). The initial direction of stress is such that each of the 22 loads has the same participation factor (both for active and reactive power) and each Northern generator participates according to speed droop;

II. *Generation to Generation* (denoted GG in the sequel): active power generation is shifted from the North ($S_{max} = 630$ MW) to the South area ($S_{max} = -600$ MW), all loads remaining unchanged. The initial direction of stress is such that Northern generators participate according to speed droop while all Southern generators have the same participation factor.

Not all α_i's and β_i's need to be treated as variables. Table 1 lists the six possible variants. For instance, in variants (a) and (c) a load power margin is determined. In variant (a), the generators' individual participations are fixed, while in variant (b) the loads' individual participations are fixed. In variant (c) both are allowed to vary. Obviously, the choice depends on the particular application. In this paper, all combinations are considered, except (a) and (c) when maximizing margins, as these variants seem less meaningful.

Table 1: margin variants

variant	transfer	α_i	$\beta_i \;\; i \in L$	$\beta_i \;\; i \in G^-$
(a)	GL	fixed	variable	= 0
(b)	GL	variable	fixed	= 0
(c)	GL	variable	variable	= 0
(d)	GG	fixed	= 0	variable
(e)	GG	variable	= 0	fixed
(f)	GG	variable	= 0	variable

The bounds B_i^+ on load power increase have been set to 10 % of the base case load. For generators, B_i^+ and B_i^- correspond to the turbine capacity.

The results shown hereafter deal with the loss of the line between buses 4011 and 4021. For a large enough North-South power transfer, this contingency causes voltage instability. If the transfer is somewhat decreased the system survives but with an overloaded line.

Thermal and voltage problems are thus strongly coupled in this example. For instance, at the thermal overload limit, some voltages are as low as 0.9 pu.

5.2 Voltage security margins

5.2.1 GL power transfer

For the initial direction of stress, the margin with respect to the selected contingency is 595 MW.

The results when optimizing the α_i's and β_i's are given in Table 2.

Table 2: bounds (MW) on voltage stability margin (GL power transfer)

variant	(a)	(b)	(c)
min margin	393	484	340
max margin	-	599	-

In variant (c), the load consumption concentrates on buses 1044, 1045, 4043, 4046, 4061 and 4051 which have the highest components of the normal vector. This load increase is covered by generators g4 and g2, whose electrical distance to the load center is higher. This corresponds to the worst direction of stress.

If only loads are varied, the generators' participations being set as indicated in the previous section, a larger minimum margin is found, as expected. Two more loads participate, at buses 4047 and 4042. If only generators are varied, the load increase is covered by g4, g2 and g3.

Note that, for voltage security analysis purposes, the identification of buses participating to the minimum load power margin carries as much information as the value of the margin itself. It points out the weak area for the contingency of concern, more precisely the smallest area in which a bounded load increase would make the system insecure with respect to the contingency.

It must be emphasized that, with the L_1-norm formulation used in this paper, if no bound B_i^- was specified on individual load increases (see (15)), the whole effort would unrealistically concentrate on a single bus. The lower the B_i^- bound, the wider the area of load increase. In variant (c), for instance, the number of loaded buses and the margin vary as follows:
- for B_i^- = 15 % of base case load: 4 buses, 330 MW ;
- for B_i^- = 10 % of base case load: 6 buses, 340 MW ;
- for B_i^- = 5 % of base case load: 21 buses, 394 MW.

Table 3 shows the ranking of load buses at 4 successive (unstable) steps of the binary search. The components of the normal vector have been scaled so that the largest one becomes equal to 1. The rows of the table are ordered according to the first normal vector obtained, while the stars point out changes with respect to this initial ranking. As can be seen, the normal vector does not change significantly from one iteration to the next. Only permutations of two successive buses are observed. Since the first ranked buses are loaded at their upper bounds B_i^- and the last ranked are not loaded at all (see Section 4.2), these permutations lead, at most, to loading one bus instead of another. The margin is little affected. Also, it is quite acceptable to use the very first vector throughout the whole procedure, which further saves computing time.

Table 3: load ranking at various steps of the binary search

stress	600MW	450MW	412MW	394MW
1044	1.0	1.0	1.0	1.0
1045	0.998	0.997	0.998	0.998
4043	0.974	0.984	0.977	0.977
4046	0.971	0.980	0.974	0.973
4061	0.967	0.973*	0.961*	0.960*
4051	0.961	0.976*	0.966*	0.965*
4047	0.947	0.963*	0.951	0.950
4042	0.946	0.963*	0.949	0.948
1043	0.939	0.932*	0.943	0.944
4041	0.938	0.955*	0.936	0.936

As regards the maximum margin (599 MW), the small difference with respect to the original margin (595 MW) is due to the small active reserve available on the most appropriate generators (by decreasing order : g11, g12, g8 and g5). The next ranked generator is g9. It has enough reserve but does not much contribute to margin increase.

5.2.2 GG power transfer

For the initial direction of stress, the margin with respect to the selected contingency is 421 MW, while the computed bounds are given in Table 4.

Table 4: bounds (MW) on voltage stability margin (GG power transfer)

variant	(d)	(e)	(f)
min margin	391	359	336
max margin	423	449	449

When generator's participations can vary in both exporting and importing areas, the smallest (voltage stability constrained) transfer of 336 MW takes place between g4, g3, g2 (North) and g7, g17 (South). This minimum is obtained by involving groups of generators electrically far away from each other.

The same Northern (resp. Southern) generators keep on participating when the Southern (resp. Northern) participations are fixed at their original values, which leads obviously to larger minimum margins.

With all participations free to vary, the maximum transaction (of 449 MW) takes place between g11, g12, g8, g5, g9 (North) and g14 alone (South). Thus, the whole effort is put on the electrically closest generators.

The maximum margins obtained when letting a single group of generators vary indicate that the generators of the importing area have less influence than those of the exporting area. This is confirmed by the margin sensitivities to injections: all Southern generators have almost the same sensitivities, while significantly larger differences are observed among the various Northern generators.

5.3 Thermal security margins

5.3.1 GL power transfer

For the initial direction of stress and taking into account thermal overloads, the margin is 535 MW. This value corresponds to the overload of line 4031-4032 after the tripping of line 4011-4021. The computed bounds are given in Table 5.

Table 5: bounds (MW) on thermal overload margin (GL power transfer)

variant	(a)	(b)	(c)
min margin	338	448	307
max margin	-	581	-

For the minimum margin of 307 MW, the load increase concentrates on buses 1043, 1044, 1045, 4042, 4043, 4046 and 4047 and is covered by g4 and g2. This load increase location causes a larger post-contingency current in line 4031-4032.

The lower bound of 448 MW involves g2 and g4, while the upper bound of 581 MW involves g11, g12, g8, g5, g21 and g22.

The lower bound of 338 MW involves the same loads as when both generation and load participations are varied.

5.3.2 GG power transfer

For the initial direction of stress, the maximum increase in power transfer is 349 MW. It is again limited by the overload of line 4031-4032 after the tripping of line 4011-4021. The computed bounds are given in Table 6.

Table 6: bounds (MW) on thermal overload margin (GG power transfer)

variant	(d)	(e)	(f)
min margin	329	305	298
max margin	384	414	437

The smallest margin of 298 MW corresponds to an increase of g2 and g4 productions, compensated by a decrease of g14.

The largest margin of 437 MW is obtained by increasing the output of generators g21, g22, g5, g8, g11 and g12 (located mainly in the left part of the network) and decreasing the output of g19. Indeed, by redirecting the pre-contingency power flow through the (double circuit) line 4031-4041, a higher transfer can take place from North to South, for the same post-contingency current in the constraining branch 4031-4032.

In this example, the limiting branch does not change when the direction of stress is modified, but the method can deal with cases where it would change.

6 CONCLUSION

This paper has presented methods for determining bounds on voltage and thermal security margins under power transfer uncertainty. These margins are defined with respect to contingencies.

Each bound is the solution of a constrained L_1-norm optimization problem. Generation and/or load powers are allowed to vary within specified limits.

Thermal overload margins are treated using linearization. A simple correction technique accounts for nonlinearities. The computation of a thermal margin bound is fast, the main effort being two (linear case) or three (with correction) contingency evaluations at some stress levels.

As far as voltage stability is concerned, the fast QSS time simulation is used to simulate contingencies and obtain the information needed to adjust the direction of stress during the bound computation. This leads to the same computational effort as for a conventional margin.

Most often the result is not only the bound but also the location of the corresponding load/generation increases.

For both types of margins, lower and upper bounds can be computed with respect to several contingencies simultaneously.

REFERENCES

[1] H.P. St. Clair, “Practical concepts in capability and performance of transmission lines”, AIEE Transactions, Vol. 72, December 1953, pp. 1152-1157

[2] O. Alsac and B. Stott, “Optimal load flow with steady-state security”, IEEE Transactions on Power Apparatus and Systems, vol. PAS-93, May/June 1974, pp. 745-751

[3] C.W. Taylor, “Power System Voltage Stability”, EPRI Power System Engineering Series, Mc Graw Hill, 1994

[4] T. Van Cutsem and C. Vournas, “Voltage Stability of Electric Power Systems”, Kluwer Academic Publisher, 1998

[5] A. J. Wood and B. F. Wollenberg, “Power generation, operation and control”, John Wiley and Sons, New York, 1996

[6] J. Jarjis and F. D. Galiana, “Quantitative analysis of steady state stability in power networks”, IEEE Transactions on Power Apparatus and Systems, Vol. PAS-100, no. 1, January 1981, pp. 318-326

[7] I. Dobson and L. Lu, “New methods for computing a closest saddle node bifurcation and worst case load power margin for voltage collapse”, IEEE Transactions on Power Systems, Vol. 8, No. 3, August 1993, pp. 905-911

[8] F. Alvarado, I. Dobson and Y. Hu, “Computation of closest bifurcations in power systems”, IEEE Transactions on Power Systems, Vol. 9, No. 2, May 1994, pp. 918-928

[9] R. Wang and R. H. Lasseter, “Re-dispatching generation to increase power system security margin and support low voltage bus”, IEEE Transactions on Power Systems, Vol. 15, No. 2, May 2000, pp. 496-501

[10] C. Vournas, M. Karystianos and N. Maratos, “Exploring power system loadability surface with optimization methods”, Proc. 5th Bulk Power Systems Dynamics and Control workshop, Onomichi (Japan), Aug. 2001, pp. 457-469

[11] I. Dobson and L. Lu, “Computing an optimum direction in control space to avoid saddle node bifurcation and voltage collapse in electric power systems”, IEEE Trans. on Automatic Control, Vol. 37, 1992, pp. 1616-1620

[12] C.A. Canizares, “Calculating optimal system parameters to maximize the distance to saddle-node bifurcations”, IEEE Trans. on Circuit and Systems-I: Fundamental theory and Applications, vol. 45, 1998, pp. 225-237

[13] D. Gan, X. Luo, D.V. Bourcier and R.J. Thomas, “Min-Max Transfer Capability: Preliminary Results”, Power Engineering Society Winter Meeting, 2001 IEEE, Vol.1, 2001, pp. 66-71

[14] T. Van Cutsem, F. Capitanescu, C. Moors, D. Lefebvre and V. Sermanson, “An advanced tool for preventive voltage security assessment”, Proc. VIIth SEPOPE conference, Curitiba (Brazil), May 2000, (invited) paper IP-035

[15] C. Moors and T. Van Cutsem, “Determination of optimal load shedding against voltage instability”, Proc. 13th PSCC, Trondheim (Norway), 1999, pp. 993-1000